Journal de Ciencia e Ingeniería, vol.15, no.1, pp. 1- 9, 2023
http://jci.uniautonoma.edu.co
DOI: https://doi.org/10.46571/JCI.2023.1.1

Journal de Ciencia e Ingeniería

Corporación Universitaria Autónoma del Cauca
ISSN 2145-2628, e-ISSN 2539-066X
Ingeniería Electrónica

Double Band MIMO Antenna Design for WLAN, IoT and LTE Applications

Diseño de una antena MIMO de doble banda para aplicaciones WLAN, IoT y LTE

Diego Pacheco-Jardiners, Gabriela Leija-Hernández and Luis Alejandro Iturri-Hinojosa
ESIME-Zacatenco, Instituto Politécnico Nacional, Col. Lindavista C.P. 07738, CDMX, México

Abstract. This paper presents a double band multiple-input multi-output (MIMO) antenna design for UWB applications, WLAN 2.4 GHz, WiMAX 3.3 – 3.6 GHz, Internet of Things (IoT) and LTE 9/24 38/41 48/52 bands. Two circular patches form the MIMO antenna array with an "I" shaped EBG structure inserted between the patch antennas to improve the isolation between elements. The The low frequency band spectrum is from 1.03 GHz to 5.03 GHz, and the high frequency band spectrum is from 6.13 GHz to 11.62 GHz. The maximum isolation between ports at 3.8 GHz and 6.9 GHz are 7 dB and 8 dB, respectively. The antenna gain at 7 GHz reaches 4.05 dB.

Keywords. MIMO antenna; EBG; WLAN; IoT and LTE.

Resumen. El artículo presenta el diseño de una antena de doble banda de múltiples entradas y múltiples salidas (MIMO) para aplicaciones UWB, WLAN de 2,4 GHz, WiMAX de 3,3 a 3,6 GHz, Internet de las cosas (IoT) y bandas LTE 9/24 38/41 48/52. Dos parches circulares forman el arreglo de antenas MIMO con una estructura EBG en forma de "I" insertada entre las antenas de parche para mejorar el aislamiento entre los elementos. El espectro de la banda de baja frecuencia es desde 1.03 GHz a 5.03 GHz, y el espectro de la banda de alta frecuencia es desde 6.13 GHz a 11.62 GHz. El aislamiento máximo entre puertos a 3.8 GHz y 6.9 GHz es de 7 dB y 8 dB, respectivamente. La ganancia de antena a 7 GHz alcanza los 4.05 dB.

Palabras Claves. Antena MIMO; EBG; WLAN; IoT y LTE.

How to cite. D. Pacheco-Jardiners, G. Leija-Hernández and A. Iturri-Hinojosa, Double band MIMO antenna design for WLAN, IoT and LTE applications. *Jou. Cie. Ing.*, vol 15, no. 1, pp. 1-9, 2023. doi:10.46571/JCI.2023.1.1

Received: 05/01/2023 **Revised:** 15/03/2023 **Accepted:** 3/05/2023

1. Introduction

In the last years, the demand for wireless communication systems has focused on information capacity, the greater rate in wireless communication, higher bandwidth, and compact antenna geometry. Also, the simultaneous requirement is increasing with the different wireless network technologies [1].

Current communication systems have multiple advantages and important properties, such as low-power networks, low-cost devices, some of them use a low level of radiated signal energy for short bandwidth and high bandwidth as UWB radio techniques [1, 2]. However, the fifth generation of the communications is closer, within the 5G we have the Internet of Things (IoT). The internet of things (IoT) is a promising technology which tends to revolutionize and connect the global world via heterogeneous smart devices through seamless connectivity [2]. IoT leads with low-power devices which interact each other through the internet. Currently there are operating technologies that have been deployed several devices worldwide, such as Bluetooth and ZigBee.

Bluetooth has been designed to operate in the 2.4 GHz ISM band with achievable data rates in the low Mbps. On the other hand, ZigBee is currently a standard for low-rate wireless personal area networks (LR-WPAN). It uses three different frequency bands: 868 MHz, 914 MHz and 2.4 GHz and a data rate of 250 kbps [3].

The Long-Term Evolution (LTE) mobile application is used for high-speed data transmission for mobile phones and one of its operating frequency band is from 2.3 GHz to 2.4 GHz. Furthermore, Wireless Local Area Networks (WLAN) with the 802.1 a/b/g/n standards of the Institute of Electrical and Electronic Engineers (IEEE) use the frequencies 2.4 GHz (2.412 GHz to 2.4835 GHz) and 5 GHz (4.9 to 5.9 GHz) [4].

The main MIMO technology requirements are good signal level, small-scale fading, and minimum mutual coupling. This technology has gained a lot of importance in the present times due to the significant advantages it provides.

In the multiple-input multiple-output (MIMO) antenna system, high isolation based on miniaturization of the antenna array has been pursued [5]. To date, several methods have been presented to reduce the MC caused by the surface currents [6]. 3-D metamaterials [7], etched parasitic elements [8, 9], defected ground structure (DGS) [10], split rings resonators (SRR) [11], neutralization line [12], Frequency Selective Surface (FSS) wall [13], Near-Field Resonator Superstrate [14] and electromagnetic bandgap (EBG) structures are some of these methods that manipulate MC by blocking, minimizing, or attenuating the surface current propagation [15–19].

The paper presents a 2x1 MIMO antenna array consisting of circular patches and an EBG structure for simultaneous operation in WLAN, LTE, and the Internet of things technologies, with resonance frequencies at 2.8 and 6.9 GHz and gain of 4.05 dB at 7 GHz.

2. Microstrip element geometry

The proposed circular patch element is designed on a FR4 epoxy substrate with relative permittivity (ε_r) equal to 4.4. The antenna parameters are circular patch radius (a), substrate length (L_s), substrate width (W_s), feed line width (L_f), feed line length (W_f), substrate thickness (h), tangential loss (δ) and substrate dielectric constant (ε_r). To calculate the circular patch radius (a), an effective radius (a_e) is required, Eq. (1), and the resonance frequency (f_{rc}) for the dominant mode TM_{110}, Eq. (2) [17].

$$a_e = a\left\{1 + \frac{2h}{\pi a \varepsilon_r}\left[ln\left(\frac{\pi a}{2h}\right) + 1.7726\right]\right\}^{0.5} \tag{1}$$

$$f_{rc} = \frac{1.8412 v_0}{2\pi a_e \sqrt{\varepsilon_r}} \tag{2}$$

where v_0 is the speed light in the free space.

A first-order approximation to the solution of Eq. (1) for the physical radio (a) is to find a_e using Eq. (2), that leads to:

$$a = \frac{F}{\left\{1 + \frac{2h}{\pi \varepsilon_r F}\left[ln\left(\frac{\pi F}{2h}\right) + 1.7726\right]\right\}^{0.5}} \tag{3}$$

where

$$F = \frac{8.791 \times 10^9}{f_r \sqrt{\varepsilon_r}} \tag{4}$$

h in Eq. (3) is in centimeters.

For 7 GHz of resonance frequency (f_r), a value of 0.606 is obtained for F with Eq. (4). The patch radius (a) results 6 mm.

$$W_f = \frac{c}{2f_r}\sqrt{\frac{2}{\varepsilon_r + 1}} \tag{5}$$

The feed line width (W_f) of the circular patch results equal to 13.16 mm using Eq. (5).

The feed line length is calculated using Eq. (6) to Eq. (9). The effective permittivity is obtained with Eq. (6).

$$\varepsilon_{\varepsilon ff} = \frac{\varepsilon_r + 1}{2} + \frac{\varepsilon_r - 1}{2}\left(\frac{1}{\sqrt{1 + \frac{10h}{W}}}\right); \frac{w}{h} > 1 \tag{6}$$

A value of 3.7 for the effective permittivity is obtained. The incremental length (ΔL) can be calculated with Eq. (7).

$$\Delta L = 0.412h\left[\frac{\varepsilon_{eff} + 0.3}{\varepsilon_{eff} - 0.258}\right]\left[\frac{\frac{W}{h} + 0.264}{\frac{W}{h} + 0.813}\right] \tag{7}$$

From Eq. (7) the incremental length is 0.72 mm. The feed line length can be calculated using Eq. (8).

$$L_f = \frac{c}{2f_r\sqrt{\varepsilon_{reff}}} - 2\Delta L \tag{8}$$

A value of 9.7 mm is obtained for the feed line length, but only 1/3 parts from this value is used to get better resonance characteristics. The ground plane length is obtained by Eq. (9).

$$L_g = \frac{c}{4f_r} \tag{9}$$

A value of 10.71 mm is obtained.

3. Circular patch antenna performance

The circular patch antenna geometry is presented. The patch, ground and feed line dimensions have been calculated by the equations described in the last section and some of them have been optimized to achieve a better performance. Fig. (1) shows the circular patch geometry.

The antenna performance was estimated by simulation of the geometry using the 3D electromagnetic simulation software HFSS by Ansys. Based on Fig. (2), the operating bandwidth is 8.45 GHz, from 1.79 GHz to 10.24 GHz, with a better impedance matching at 4.7 GHz and 8.6 GHz.

The radiation pattern in E and H planes is shown in Fig. (3). Fig. (4) shows the radiation pattern in 3 dimensions with gain values included in decibels. At 7 GHz the gain is 3.35 dB.

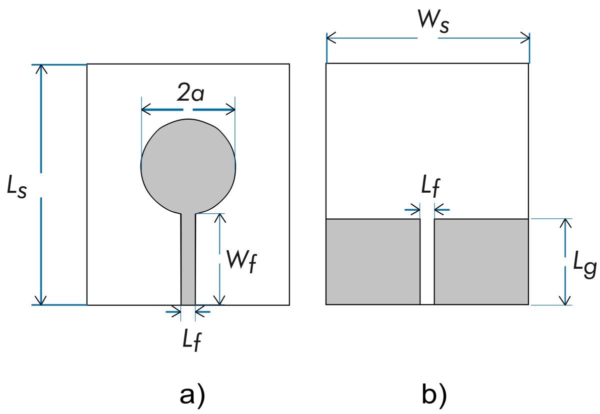

Figure 1: Circular Patch antenna geometry (a) top view and (b) bottom view. Units in millimetres.

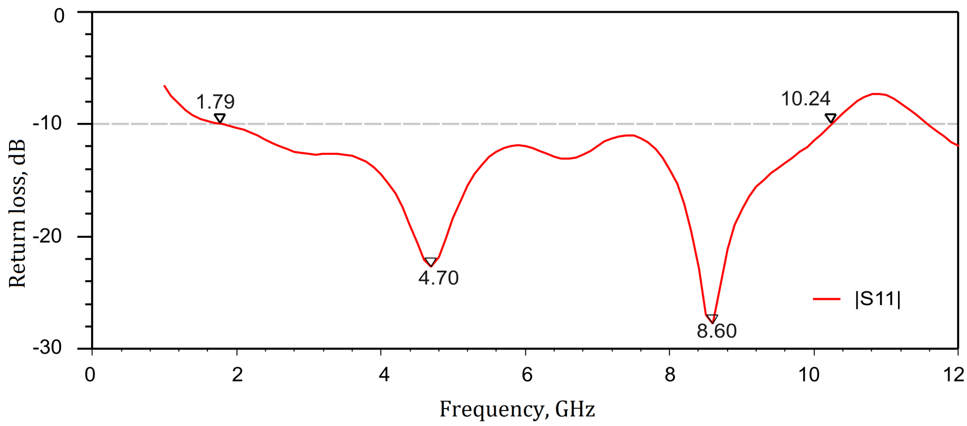

Figure 2: Return loss of the circular patch antenna.

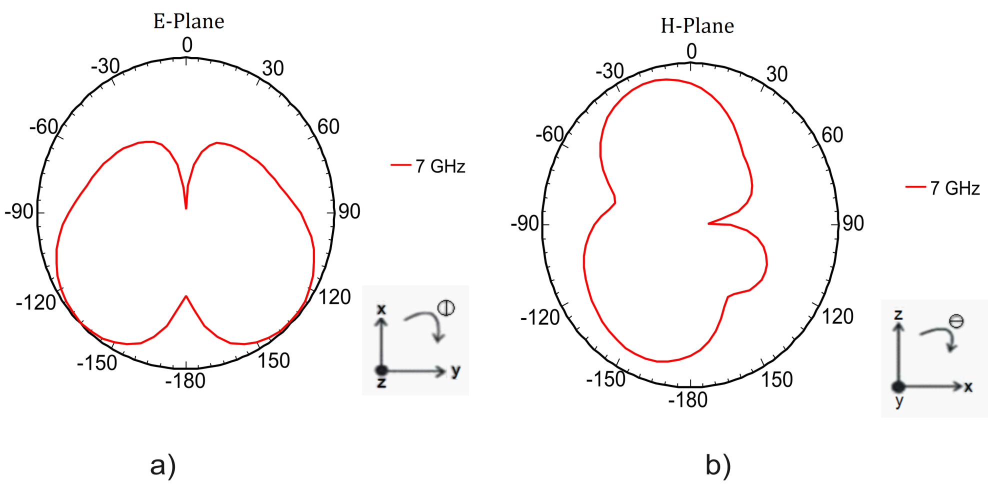

Figure 3: Radiation Pattern in (a) E Plane and (b) H Plane at 7 GHz.

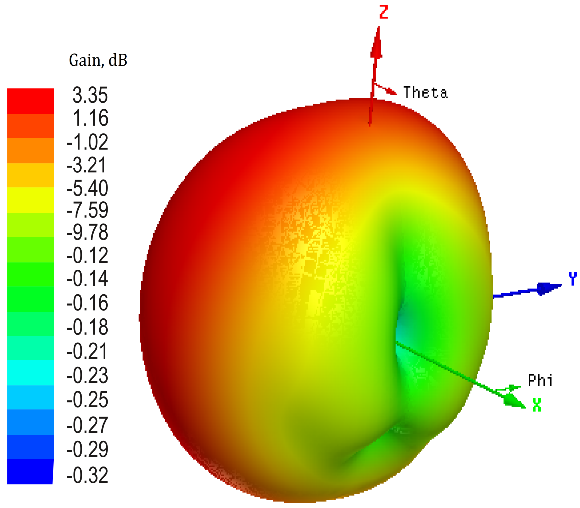

Figure 4: 3D radiation gain of the circular patch element.

4. 2X1 MIMO array antenna without EBG structure

The geometry of the proposed UWB MIMO antenna without EBG is shown in Fig. (5). Proposed UWB MIMO antenna is printed on a 50 mm × 84 mm × 1.6 mm FR4 substrate with relative permittivity equal to 4.4 and a loss tangent of 0.02. A 3 mm width, 50Ω microstrip line is used for feeding the identical antenna elements. The feed line used in this design is known as "taper" [3], it has an increasing width towards to the SMA connector and is used as impedance transformer.

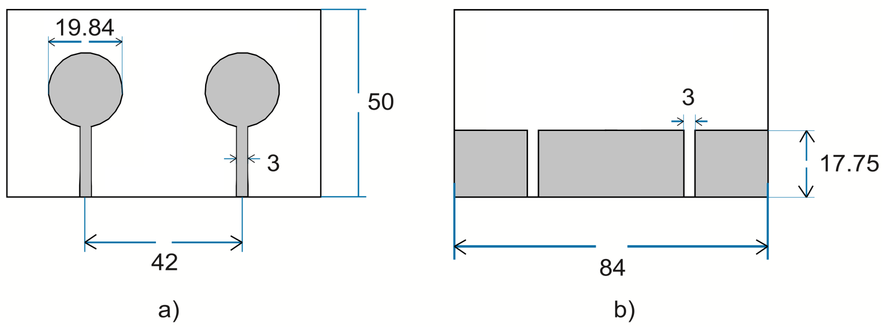

Figure 5: 2x1 MIMO antenna geometry (a) top view and (b) bottom view. Units in millimetres.

The transmission (S_21) and reflection (S_11) coefficients for the 2x1 MIMO antenna are shown in Fig. (6). The simulated -10 dB impedance bandwidth of antenna is 10.71 GHz (1.29 GHz - 12 GHz). The maximum resonance frequencies occur at 3.8 GHz, 6.9 GHz, and 10.1 GHz. The mutual coupling is higher than -15 dB at all the resonance frequencies. Fig. (7) shows the radiation patterns in E and H planes. Fig. (8) shows the radiation pattern in 3D including gain values in decibels at 7 GHz. A 4.47 dB peak gain is estimated.

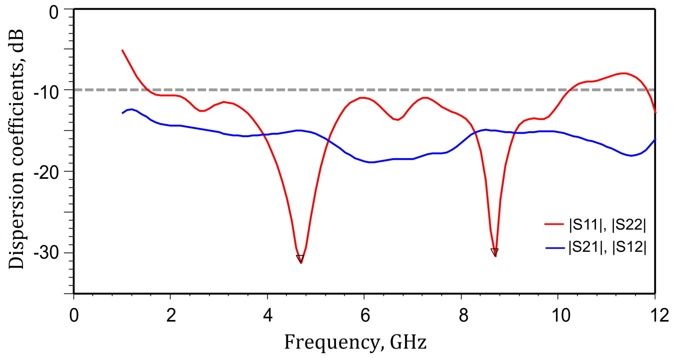

Figure 6: Simulated return loss and transmission coefficient of the antenna without EBG structure.

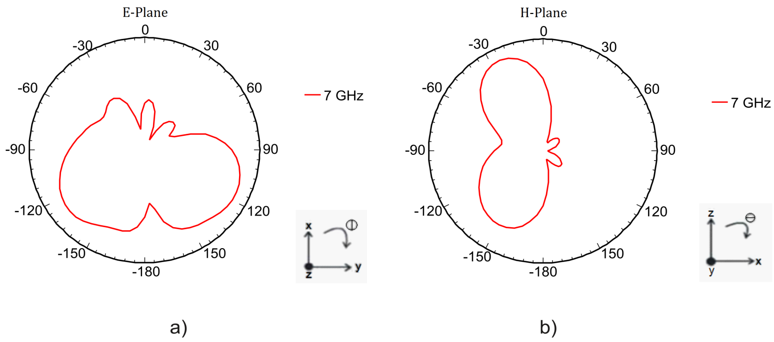

Figure 7: Radiation pattern in (a) E and (b) H -planes at 7 GHz.

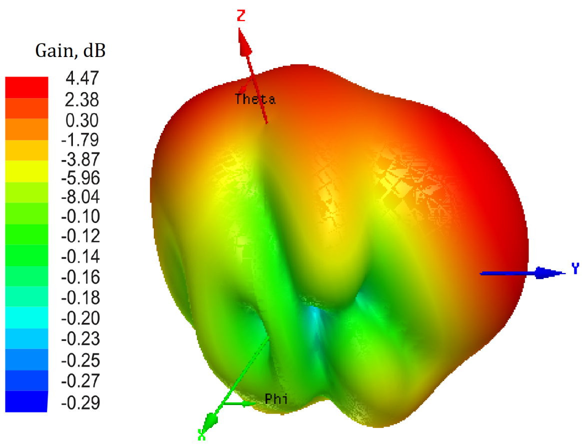

Figure 8: 3D radiation gain of MIMO antenna without EBF structure.

5. 2x1 MIMO array antenna with EBG Structure

An "I" shape EBG structure between the antenna elements was inserted. The EBG structure is formed by two horizontal microstrips, the upper segment is 2 mm width and 60 mm length, the lower segment 2 mm width and 30 mm length and the vertical microstrip is 3 mm width. A defected ground structure was used to achieve performance enhancements. Fig. 9 shows the 2x1 MIMO antenna geometry with the EBG structure. The proposed antenna uses 1.6 mm thick, low cost FR4 substrate, possessing an overall size of 50 mm × 84 mm.

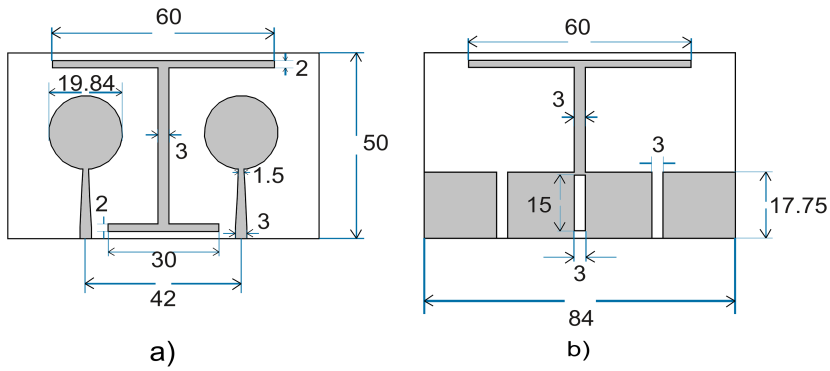

Figure 9: 2x1 MIMO antenna geometry with EBG structure (a) top view and (b) bottom view. Units in millimeters.

The transmission (S_21) and reflection (S_11) coefficients, both in decibels, are shown in Fig. (10).

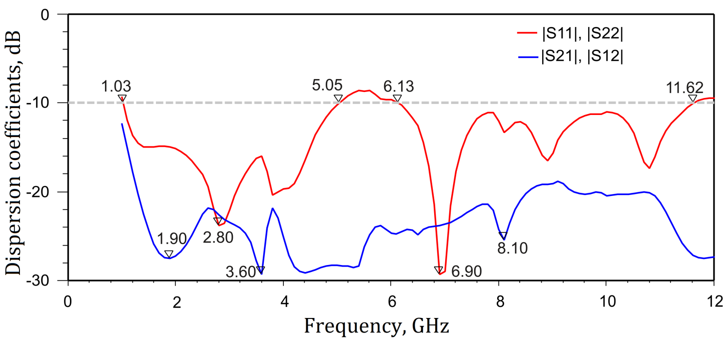

Figure 10: Simulated return loss and transmission coefficient of the Antenna with EBG structure.

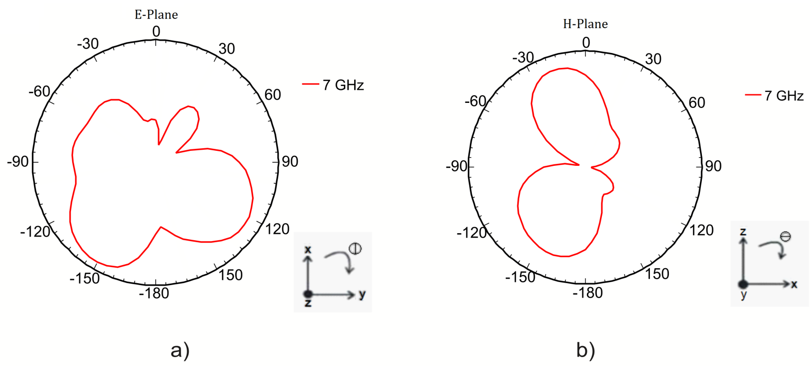

Figure 11: Radiation pattern in (a) E and (b) H -plane at 7 GHz.

Two resonance frequencies are exhibited at 2.8 and 6.9 GHz, and two operating frequency bands, a lower band of 4 GHz (1.03 - 5.03 GHz) and high band of 5.49 GHz (6.13 - 11.62 GHz).

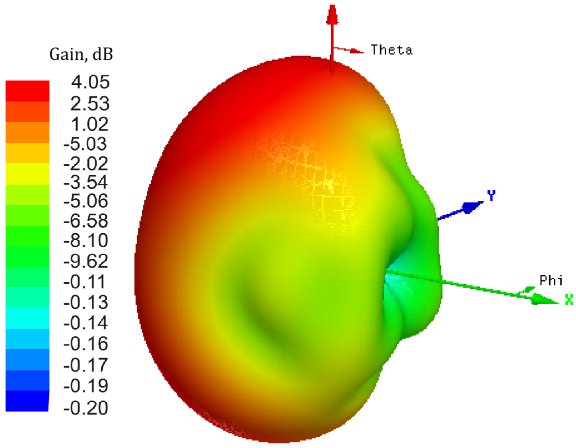

Figure 12: Total gain and radiation pattern in 3D for the MIMO antenna with EBG structure.

The mutual coupling improvement is about 7 and 8 dB at 3.8 and 6.9 GHz, respectively. In both operating bands, mutual coupling is below -18 dB. Radiation patterns in E and H -planes and the 3D radiation gain were simulated and are shown in Fig. (11) and Fig. (12). A maximum 4.05 dB at 7 dB is perceived.

6. Conclusions

A WLAN, IoT and LTE 2x1 MIMO antenna with EBG structure is proposed. The MIMO antenna has dimensions of 50 mm x 84 mm. An impedance transformer was used to improve the patch and feed point coupling. The simulated -10 dB impedance bandwidth of antenna without EBG structure is 10.71 GHz (1.29 - 12 GHz) and that of antenna loaded with EBG has a low-band spectrum from 1.03 GHz to 5.03 GHz (4 GHz) and high-band spectrum from 6.13 GHz to 11.62 GHz (5.49 GHz). At 3.8 and 6.9 GHz the mutual coupling improvement was just about 7 and 8 dB, respectively. And a gain of 4.05 dB is achieved.

Acknowledgements

The authors express thanks to the support received by the project SIP20221930.

References

[1] Anusudha, K., & Karmugil, M. (2016, December). Design of circular microstip patch antenna for ultra wide band applications. In 2016 International Conference on Control, Instrumentation, Communication and Computational Technologies (ICCICCT) (pp. 304-308). IEEE.

[2] D. Castro Carreras, "Diseño e implementación de antenas MIMO de banda ancha con filtros de rechazo de bandas", Bachelor's Thesis, Univ. Aut. Madrid, 2019 [Online]. Avaible: http://hdl.handle.net/10486/689014.

[3] G. A. Akpakwu, B. J. Silva, G. P. Hancke and A. M. Abu-Mahfouz, "A Survey on 5G Networks for the Internet of Things: Communication Technologies and Challenges," in IEEE Access, vol. 6, pp. 3619-3647, 2018, doi: 10.1109/ACCESS.2017.2779844.

[4] F. Palacios et al., "Circular Patch Antenna for Ultra Wide Band Applications", World Engineering & Applied Sciences Journal 10 (2), 2019, pp. 58-60, doi: 10.5829/idosi.weasj.2019.58.60.

[5] Z. U. Abedin. "Circular Microstrip Patch Antenna Design for LTE, ISM, WIMAX, Satellite Communication and in Ultra Wideband Applications", in International Conference on Broadband and Wireless Computing, Communication and Applications, Springer, Cham, pp. 718-727, 2017.

[6] Wireless Medium Access Control and Physical Layer Specifications for Low-Rate Wireless Personal Area Networks, IEEE Standard 802.15.4, IW Group, 2003.

[7] Guo, J. Y., Liu, F., Jing, G. D., Zhao, L. Y., Yin, Y. Z., & Huang, G. L. (2020). Mutual coupling reduction of multiple antenna systems. Frontiers of Information Technology & Electronic Engineering, 21, 366-376.

[8] Chouhan S, Panda DK, Gupta M, Singhal S. Multiport MIMO antennas with mutual coupling reduction techniques for modern wireless transreceive operations: a review. Int J RF Microwave Comput Aided Eng 2018;28(2): e21189.

[9] Yu K, Li Y, Liu X. Mutual coupling reduction of a MIMO antenna array using 3-D novel meta-material structures. Appl Computat Electromagnet Soc J 2018;33 (7):758–63.

[10] Sun XB, Cao MY. Mutual coupling reduction in an antenna array by using two parasitic microstrips. AEU-Int J Electron Commun 2017;74:1–4.

[11] Zaker R. Design of a very closely-spaced antenna array with a high reduction of mutual coupling using novel parasitic L-shaped strips. Int J RF Microwave Comput Aided Eng 2018;28(9):e21422.

[12] Xiao S, Tang MC, Bai YY, Gao S, Wang BZ. Mutual coupling suppression in microstrip array using defected ground structure. IET Microwaves Antennas Propag 2011;5(12):1488–94.

[13] Sahandabadi S, Makki SVAD. Mutual coupling reduction using complementary of SRR with wire MNG structure. Microwave Opt Technol Lett 2019;61(5):1231–4.

[14] Zhang S, Pedersen GF. Mutual coupling reduction for UWB MIMO antennas with a wideband neutralization line. IEEE Antennas Wirel Propag Lett 2015; 15:166–9.

[15] Beiranvand E, Afsahy M, Sharbati V. Reduction of the mutual coupling in patch antenna arrays based on EBG by using a planar frequency-selective surface structure. Int J Microwave Wireless Technolog 2017;9(2):349–55.

[16] Li M, Zhong BG, Cheung SW. Isolation enhancement for MIMO patch antennas using near-field resonators as coupling-mode transducers. IEEE Trans Antennas Propag 2018;67(2):755–64.

[17] Balanis, C. A., *Antenna theory: analysis and design*, John wiley & sons, 2016, pp. 843-852.

[18] Biswas AK, Chakraborty U. Reduced mutual coupling of compact MIMO antenna designed for WLAN and WiMAX applications. Int J RF Microwave Comput Aided Eng 2019;29(3): e21629.

[19] Abdelgwad AH, Ali M. Isolation improvement of a two-port PIFA for MIMO using a planar EBG ground. Microwave Opt Technol Lett 2020;62(2):737–42.